

# The nonmonotonic dose dependence of optically stimulated luminescence in $\text{Al}_2\text{O}_3:\text{C}$ : Analytical and numerical simulation results

R. Chen<sup>a)</sup>

*School of Physics and Astronomy, Raymond and Beverly Sackler Faculty of Exact Sciences, Tel-Aviv University, Tel-Aviv 69978, Israel*

V. Pagonis

*Physics Department, McDaniel College, Westminster, Maryland 21157*

J. L. Lawless

*Redwood Scientific Inc., Pacifica, California 94044*

(Received 2 September 2005; accepted 8 December 2005; published online 7 February 2006)

Nonmonotonic dose dependence of optically stimulated luminescence (OSL) has been reported in a number of materials including  $\text{Al}_2\text{O}_3:\text{C}$  which is one of the main dosimetric materials. In a recent work, the nonmonotonic effect has been shown to result, under certain circumstances, from the competition either during excitation or during readout between trapping states or recombination centers. In the present work, we report on a study of the effect in a more concrete framework of two trapping states and two kinds of recombination centers involved in the luminescence processes in  $\text{Al}_2\text{O}_3:\text{C}$ . Using sets of trapping parameters, based on available experimental data, previously utilized to explain the nonmonotonic dose dependence of thermoluminescence including nonzero initial occupancies of recombination centers ( $\text{F}^+$  centers), the OSL along with the occupancies of the relevant traps and centers are simulated numerically. The connection between these different resulting quantities is discussed, giving a better insight as to the ranges of the increase and decrease of the integral OSL as a function of dose, as well as the constant equilibrium value occurring at high doses. © 2006 American Institute of Physics. [DOI: [10.1063/1.2168266](https://doi.org/10.1063/1.2168266)]

## I. INTRODUCTION

Optically stimulated luminescence (OSL) is the effect of light emission during exposure of a solid sample to stimulating light (usually of different wavelength) following an irradiation by, say,  $\beta$  rays,  $\gamma$  rays, or x rays. The effect is understood to be the result of absorption of energy during the ionizing radiation exposure, part of which can be released in the form of measurable light while illuminating the sample by light of a different wavelength. The effect is similar to thermoluminescence (TL), in which the excitation stage is exactly the same, but the trigger for releasing the absorbed energy is the heating of the sample. Both TL and OSL are used for dosimetry, which can be employed when the measured luminescence is a simple increasing monotonic function of the dose, preferably linear. The possible superlinearity and sublinearity of these effects have been discussed elsewhere.<sup>1</sup> In several materials, the dose dependence of TL has been found to be an increasing function at low doses, reached a maximum at a certain dose, and declined at higher doses, sometimes leveling off at a certain high dose. Some authors ascribed this effect to “radiation damage” though no details were given. A review of the experimental evidence of this effect in TL as well as a theoretical account has been given by Lawless *et al.*<sup>2</sup> The explanation of the nonmonotonic dose dependence in TL was given in terms of competition between transitions into active and competing traps or

between radiative and nonradiative recombination centers. Competitions during the excitation stage or the heating, readout stage have been considered.

Schulman *et al.*<sup>3</sup> described the changes in photoluminescence due to prior  $\gamma$  excitation in organic solids, which in our present terms can be understood to be OSL. For example, in naphthalene, the dependence of 464 nm emission stimulated by 365 nm UV light depended nonlinearly on the previous  $\gamma$ -excitation dose, reaching a maximum at  $\sim 10^5$  Gy and decreasing at higher doses. Since the stimulating wavelength is shorter than that of the emitted light, one might think that this is simply photoluminescence; however, this is obviously not the case since the role of the initial  $\gamma$  irradiation is crucial. Freytag,<sup>4</sup> Tesch,<sup>5</sup> and Böhm *et al.*<sup>6</sup> described the  $\gamma$ -dose dependence of silver-activated phosphor glass which is used for dose measurements. The effect was termed by these authors radiophotoluminescence (RPL). A visible orange light stimulated by 365 nm UV light was found to increase linearly with the prior applied  $\gamma$  dose between  $10^{-2}$  and  $10^2$  Gy, reached a maximum at  $\sim 3 \times 10^3$  Gy, and declined by nearly three orders of magnitude at higher doses up to  $10^8$  Gy. The strict linearity with the dose between  $10^{-2}$  and 50 Gy enables the evaluation of the dose in this region. Freytag<sup>4</sup> has pointed out that the region of decreasing RPL could also be used for dose measurements, provided a well-determined curve is available. Zeneli *et al.*<sup>7</sup> have further studied the behavior of radiophotoluminescent glasses which, as they report, is being used for high-level dosimetry around the particle accelerators. These authors also studied the light emission by 365 nm stimulation following  $\gamma$  irra-

<sup>a)</sup>Electronic mail: chenr@tau.ac.il

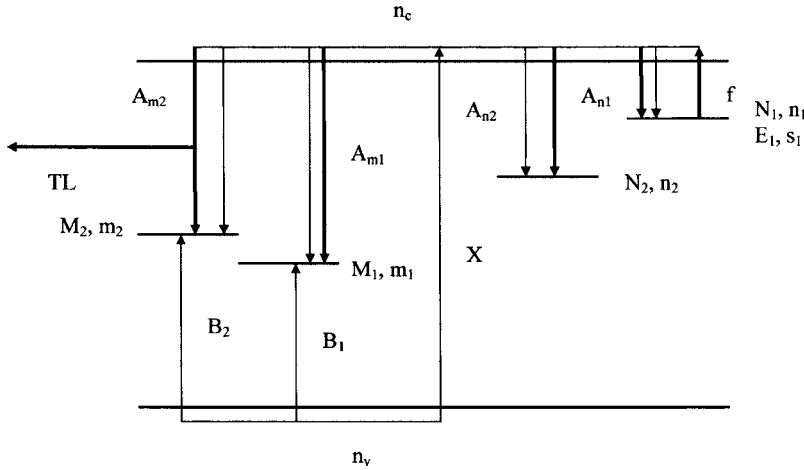


FIG. 1. The energy-level diagram of two electron trapping states and two kinds of hole recombination centers. Transitions occurring during excitation are given by the solid lines, and transitions taking place during the optical readout stage are shown by the thick lines.

radiation. They reported on a  $\gamma$ -dose dependence which was a nearly linear function between  $10^{-1}$  and  $10^2$  Gy, reached a maximum at  $\sim 10^3$  Gy, and declined substantially at doses up to  $10^6$  Gy at all the temperatures used, namely, 4.6, 77, and 300 K. The authors ascribed the decline to the self-absorption of the luminescent light.

An important material in which the nonmonotonic effect of both TL and OSL has been observed is  $\text{Al}_2\text{O}_3$  with or without C impurities. Bloom *et al.*<sup>8</sup> studied pulsed OSL (POSL) in  $\text{Al}_2\text{O}_3$  single crystals and reported a small decline of POSL at  $\beta$  doses above  $\sim 10$  Gy. Yukihiro *et al.*<sup>9</sup> described a model of two trapping states and two kinds of recombination centers pertinent to  $\text{Al}_2\text{O}_3:\text{C}$  and discussed the character and concentrations of the traps and centers. In particular, the concentration of preexisting  $\text{F}^+$  centers which is likely to be many orders of magnitude higher than the radiation-induced  $\text{F}^+$  centers appears to be of great importance.<sup>10</sup> Yukihiro *et al.*<sup>11,12</sup> reported on the nonmonotonic dose dependence of OSL in  $\beta$ -irradiated  $\text{Al}_2\text{O}_3:\text{C}$ . Both integrated cw-OSL and initial OSL were found to reach a maximum which, depending on the sample, often occurred at  $\sim 35$  Gy of  $\beta$  excitation, the effect being somewhat stronger in the latter than in the former. In parallel, the measurements revealed a maximum in the dose dependence of TL at about the same dose. Pagonis *et al.*<sup>13</sup> simulated the nonmonotonic dose dependence of TL in  $\text{Al}_2\text{O}_3:\text{C}$  using different sets of trapping parameters, some of which previously suggested by McKeever *et al.*<sup>10</sup> and Yukihiro *et al.*<sup>11,12</sup> For three different  $\text{Al}_2\text{O}_3:\text{C}$  samples labeled “chip 101,” “B1040,” and “D320,” the TL results varied to some extent, and the parameters were adjusted to fit these results. The dependence of the linear absorption coefficient on the dose was also simulated and compared to the data by Yukihiro *et al.*<sup>9</sup>

In the present work, we simulate the dependence of the integrated OSL on the dose with the same set of parameters related to the sample labeled chip 101 mentioned by Pagonis *et al.*<sup>14</sup> The calculations follow a previous work by Chen and Leung<sup>15</sup> dealing with a much simpler model of one trapping state and one kind of recombination center, and with pulsed OSL. Preliminary results have been given by Pagonis *et al.*,<sup>14</sup> but in the present work we get a much better insight into the conditions between the active center occupancy before and

after the stimulation and the peak shape of the OSL dependence on the dose. The initial increase and later decrease of the integral OSL with the dose are explained in terms of the relation between the concentrations of trapping states, recombination centers, and the initial, radiation-independent, concentration of the active luminescence center ( $\text{F}^+$ ). Also, the constant plateau value of the integral OSL reached at high doses is also explained using the same concentrations.

## II. THE MODEL AND RELEVANT SET OF PARAMETERS

The model used is shown in Fig. 1, and is rather similar to that given by Yukihiro *et al.*<sup>9</sup> Two trapping states are taken into consideration,  $N_1$  which is an “active” dosimetric trap, meaning that the stimulating light is capable of releasing electrons from it, and  $N_2$ , a competitor in which electrons can be trapped, but the stimulating light cannot release electrons from it. Two recombination centers are assumed to exist,  $M_1$  which is radiative and  $M_2$ , a nonradiative competitor. The set of six coupled differential equations governing the process during excitation is

$$\frac{dm_1}{dt} = -A_{m_1}m_1n_c + B_1(M_1 - m_1)n_v, \quad (1)$$

$$\frac{dm_2}{dt} = -A_{m_2}m_2n_c + B_2(M_2 - m_2)n_v, \quad (2)$$

$$\frac{dn_1}{dt} = -sn_1 \exp(-E/kT) + A_{n_1}(N_1 - n_1)n_c, \quad (3)$$

$$\frac{dn_2}{dt} = A_{n_2}(N_2 - n_2)n_c, \quad (4)$$

$$\frac{dn_v}{dt} = X - B_2(M_2 - m_2)n_v - B_1(M_1 - m_1)n_v, \quad (5)$$

$$\frac{dn_c}{dt} = \frac{dm_1}{dt} + \frac{dm_2}{dt} + \frac{dn_v}{dt} - \frac{dn_1}{dt} - \frac{dn_2}{dt}. \quad (6)$$

Here,  $M_1$  ( $\text{cm}^{-3}$ ) is the concentration of radiative hole centers with instantaneous occupancy of  $m_1$  ( $\text{cm}^{-3}$ ),  $M_2$  ( $\text{cm}^{-3}$ )

is the concentration of nonradiative hole centers with instantaneous occupancy of  $m_2$  ( $\text{cm}^{-3}$ ),  $N_1$  ( $\text{cm}^{-3}$ ) is the concentration of the electron active trapping state with instantaneous occupancy of  $n_1$  ( $\text{cm}^{-3}$ ), and  $N_2$  ( $\text{cm}^{-3}$ ) is the concentration of the trapping state with instantaneous occupancy of  $n_2$  ( $\text{cm}^{-3}$ ).  $n_c$  and  $n_v$  are the concentrations ( $\text{cm}^{-3}$ ) of the electrons and holes in the conduction and valence bands, respectively.  $X$  ( $\text{cm}^{-3} \text{s}^{-1}$ ) is the rate of production of electron-hole pairs, which is proportional to the excitation dose rate, and  $B_1$  and  $B_2$  ( $\text{cm}^3 \text{s}^{-1}$ ) are the trapping probability coefficients of free holes in centers 1 and 2, respectively.  $A_{m_1}$  and  $A_{m_2}$  ( $\text{cm}^3 \text{s}^{-1}$ ) are the recombination probability coefficients for free electrons with holes in centers 1 and 2, and  $A_{n_1}$  ( $\text{cm}^3 \text{s}^{-1}$ ) is the retrapping probability coefficient of free electrons into the active trapping state  $N_1$ .  $A_{n_2}$  ( $\text{cm}^3 \text{s}^{-1}$ ) is the trapping probability coefficient of the free electrons into the competing trapping state  $N_2$ . If we denote the time of excitation by  $t_D$  and the rate of production of electron-hole pairs per  $\text{cm}^3$  by  $X$ , then  $Xt_D$  represents the total concentration of electrons and holes produced, which is proportional to the total dose imparted.

Concerning the values of the relevant parameters in  $\text{Al}_2\text{O}_3:\text{C}$ , these have been evaluated by Pagonis *et al.*,<sup>14</sup> based on the results by Yukihiro *et al.*,<sup>9</sup> and will be used here for OSL. We selected a four-level model of alumina that includes one dosimetric trap ( $N_1$ ), one deep electron trap ( $N_2$ ), one radiative recombination center ( $M_1$ ), and one radiationless center ( $M_2$ ). Measurements on chip 101 show that, before irradiation, the recombination center has a non-zero initial carrier concentration and that this concentration decreases

at doses above 10 Gy. We were able to reproduce this and other observed behaviors of this sample<sup>14</sup> with the following parameter set:  $M_1=10^{17} \text{ cm}^{-3}$ ,  $M_2=2.4 \times 10^{16} \text{ cm}^{-3}$ ,  $N_1=2 \times 10^{15} \text{ cm}^{-3}$ ,  $N_2=2 \times 10^{15} \text{ cm}^{-3}$ ,  $A_{m_1}=4 \times 10^{-8} \text{ cm}^3 \text{ s}^{-1}$ ,  $A_{m_2}=5 \times 10^{-11} \text{ cm}^3 \text{ s}^{-1}$ ,  $B_1=10^{-8} \text{ cm}^3 \text{ s}^{-1}$ ,  $B_2=4 \times 10^{-9} \text{ cm}^3 \text{ s}^{-1}$ ,  $A_{n_1}=2 \times 10^{-8} \text{ cm}^3 \text{ s}^{-1}$ ,  $A_{n_2}=2 \times 10^{-9} \text{ cm}^3 \text{ s}^{-1}$ ,  $X=1.7 \times 10^{15} \text{ cm}^{-3} \text{ s}^{-1}$ , and  $m_{10}=9.4 \times 10^{15} \text{ cm}^{-3}$ . The rest of the initial carrier concentrations in the model are taken equal to zero. The chosen values for  $M_1$  and  $m_{10}$  are in agreement with independent measurements inferred from optical-absorption data (Yukihiro *et al.*<sup>9</sup>). Note also that the selected rate constant values were all chosen to be within the range of commonly observed electron capture in solids (see, e.g., Lax<sup>16</sup>).

In the next stage of the process, a relaxation period has been simulated by setting the excitation dose rate to zero and solving the same set of equations for a certain period of time so as to have the concentrations of the free electrons,  $n_c$ , and free holes,  $n_v$ , go to negligible values; the initial values of the concentration functions for the relaxation stage are the final values at the excitation stage. Finally, the following five simultaneous equations are to be solved for the stimulation stage:

$$\frac{dn_1}{dt} = -fn_1 + A_{n_1}(N_1 - n_1)n_c, \quad (7)$$

$$\frac{dn_2}{dt} = A_{n_2}(N_2 - n_2)n_c, \quad (8)$$

$$\frac{dm_1}{dt} = -A_{m_1}m_1n_c, \quad (9)$$

$$\frac{dm_2}{dt} = -A_{m_2}m_2n_c, \quad (10)$$

$$\frac{dn_1}{dt} + \frac{dn_2}{dt} + \frac{dn_c}{dt} = \frac{dm_1}{dt} + \frac{dm_2}{dt}. \quad (11)$$

Here,  $f(\text{s}^{-1})$  is a magnitude proportional to the stimulating light intensity, and has been given the value of  $1/60 \text{ s}^{-1}$ . The model assumes that the stimulating light does not raise electrons from the competing trap  $N_2$ . The OSL intensity is associated with the recombination into  $m_1$ , therefore, the intensity  $I(t)$  is

$$I(t) = A_{m_1}m_1n_c. \quad (12)$$

It should be noted that, whereas in the work on TL, the maximum intensity was usually taken as the TL signal, here we prefer to follow the experimental practice in which one usually considers the integral on the decaying OSL curve over a certain period of time. It should be noted that the dose dependence may be different when a response to a short pulse of light is considered as discussed by Chen and Leung.<sup>15</sup>

The MATLAB ode23s solver as well as the MATHEMATICA solver have been used to solve numerically the relevant sets of equations, and the results reached with both were in excellent agreement. In order to evaluate the area under the OSL decaying curve, one should usually perform a numerical integration for a certain period of time along the curve. In order to bypass this step, we chose the following method. If we assume, as we did, that  $m_1$  is the hole concentration in the luminescent center, obviously the OSL intensity is  $I(t) = -dm_1/dt$ . The integral over time between zero and the chosen final time  $t_f$  yields

$$\int_0^{t_f} I(t)dt = m_{10} - m_{1f}. \quad (13)$$

We can, therefore, perform the simulation along the stimulation time, but instead of integrating over  $I(t)$ , just take the difference between the initial and final values of  $m_1$ . This method, which saves computation time, also enables a better understanding of the results as discussed below.

### III. NUMERICAL RESULTS

With the set of parameters relevant, in particular, to the  $\text{Al}_2\text{O}_3:\text{C}$  samples mentioned above, we have performed the following simulations. Different lengths of excitation were used and  $n_1$ ,  $n_2$ ,  $m_1$ , and  $m_2$  were recorded at the end of excitation plus relaxation, and plots of these magnitudes as a function of dose were made. For  $m_1$ , its value following the next stimulation stage was found for each dose, as well as the value of the integral OSL as described above [Eq. (13)].

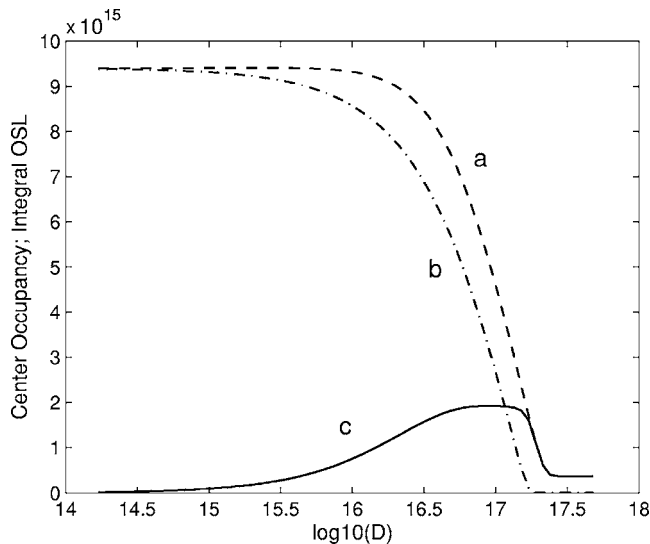


FIG. 2. Simulated dose dependence of the concentration of the occupancy of the radiative center at the end of irradiation plus relaxation (a) and the end of light stimulation (b). Curve (c) shows, under the same circumstances, the integral OSL as a function of the dose. The relevant set of parameters is given in the text and includes an initial concentration of radiative center,  $m_{10} = 9.4 \times 10^{15} \text{ cm}^{-3}$ .

Figure 2 depicts, in curve (a), the dependence of the occupancy of the radiative center,  $m_1$ , at the end of the relaxation period, on the dose. At low doses, the concentration starts at the initial value of  $9.4 \times 10^{15} \text{ cm}^{-3}$ , reduces at higher doses due to recombinations that take place during excitation, and gets to an equilibrium final value of  $\sim 3.7 \times 10^{14} \text{ cm}^{-3}$  at high doses. The significance of this equilibrium value will be discussed below in connection with the other relevant parameters of the given problem. Curve (b) shows the values of  $m_1$  for the same problem and the set of parameters, but at the end of the stimulation stage. Note that at high doses, the  $m_1$  value here reduces to practically zero, in agreement with the experimental findings of Yukihiro *et al.*<sup>11</sup> for chip 101. Curve (c) depicts the difference between the values of (a) and (b), and as explained above, it represents the area under the OSL curve as a function of the dose. The peak shape resembles, at least qualitatively, the behavior reported by Yukihiro *et al.*<sup>11</sup> for chip 101. At high doses, the OSL intensity reaches a plateau, again similarly to the experimental results. The equilibrium OSL value reached is the same value of  $\sim 3.7 \times 10^{14} \text{ cm}^{-3}$ , and the reason for this is that  $m_1$  reduces to very small values following the stimulation period.

While considering these results, we would like to compare from a different point of view the filling of the trapping states and recombination centers with the dose, with the total OSL dose dependence. Curve (a) in Fig. 3 shows, again, the dependence of the concentration of the active center at the end of relaxation as a function of dose. Curve (b) shows the increase of the active trap concentration  $n_1$  at the end of relaxation, with the dose, from an initial value of zero to a full saturation at  $2 \times 10^{15} \text{ cm}^{-3}$ .  $n_1$  reaches a saturation at a “dose” of  $\sim 10^{17} \text{ cm}^{-3}$ . Not shown here is the approach to saturation of the competitor at high doses;  $n_2$  reaches a saturation value ( $n_2 \approx N_2$ ) of  $2 \times 10^{15} \text{ cm}^{-3}$  at a simulated dose of

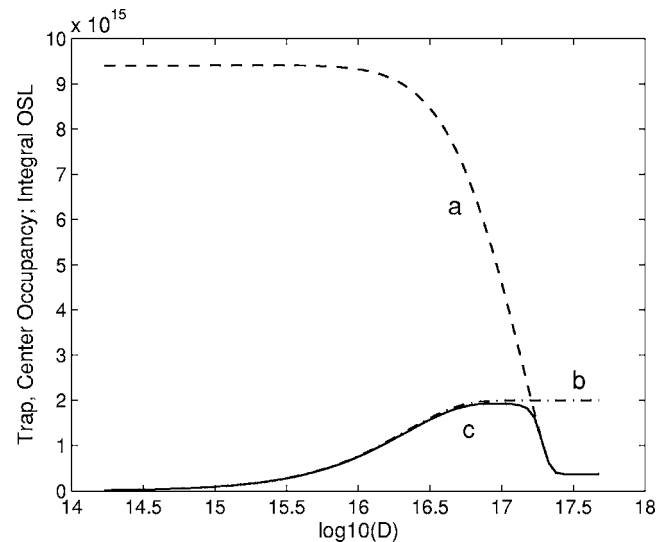


FIG. 3. With the same parameters as in Fig. 2, the occupancy of the radiative center following excitation and relaxation is shown in (a), and that of active trap in (b). Curve (c) shows the simulated integral OSL in the same range of doses.

$\sim 2.5 \times 10^{17} \text{ cm}^{-3}$ . The calculated values of the integral OSL are repeated in curve (c); the relation between these three quantities will be discussed in the next section.

Although the present work deals mainly with the behavior of the  $\text{Al}_2\text{O}_3:\text{C}$  samples, more simulations have been performed which help in getting a better insight into the processes taking place and the inter-relation between the trapping states and recombination centers. Figure 4 shows the dose dependence of  $n_1$  and  $m_1$  as a function of the dose in the same system with the same trapping parameters, except that the initial value of  $m_1$  is set to zero. This is similar to the case of sample B1040 reported by Yukihiro *et al.*<sup>9</sup> In curve (a),  $m_1$  gets to a maximum value at  $\sim 1.6 \times 10^{16} \text{ cm}^{-3}$  and then declines and remains at a plateau level of  $\sim 6.13 \times 10^{13} \text{ cm}^{-3}$  at high doses. In curve (b),  $n_1$  is seen to increase from zero to its saturation value of  $2 \times 10^{15} \text{ cm}^{-3}$ . Curve (c)

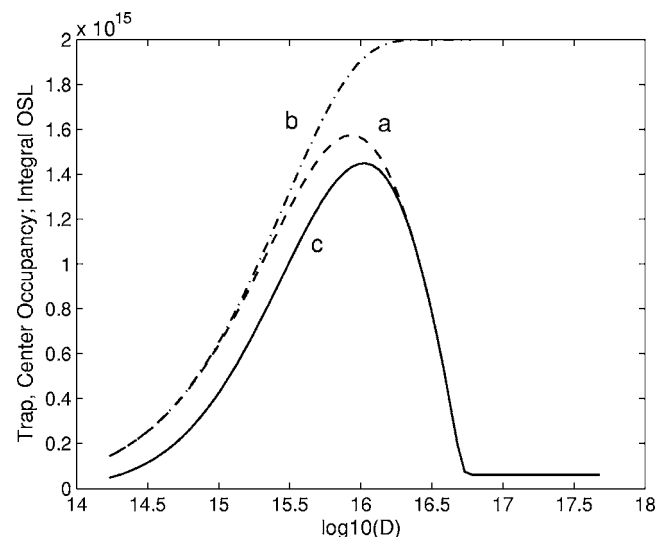


FIG. 4. Same as Fig. 3, but with  $m_{10} = 0$ . Curves (a) and (b) show, respectively, the occupancies of  $m_{10}$  and  $n_{10}$  at the end of relaxation, and (c) depicts the simulated integral OSL.

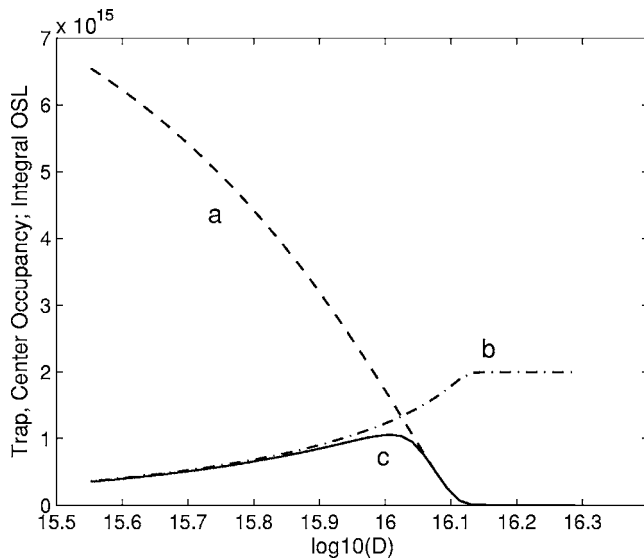


FIG. 5. Similar to Fig. 3, but the total concentration of competing centers is set to be  $M_2 = 2.4 \times 10^{18} \text{ cm}^{-3}$ .

represents the integral OSL which, roughly speaking, has a similar peak shape as  $m_1$ , but slightly shifted to higher doses. The OSL also reaches the same plateau level of  $\sim 6.13 \times 10^{13} \text{ cm}^{-3}$  as can easily be understood. These relations will also be discussed below.

Figure 5 shows the same magnitudes as Figs. 3 and 4 but the capacity of the competitor center is increased by two orders of magnitude to be  $2.4 \times 10^{18} \text{ cm}^{-3}$ ; the initial value of  $m_1$  is  $9.4 \times 10^{15} \text{ cm}^{-3}$  as in Fig. 3. Here too, the behavior at low doses resembles that of the dose dependence of  $n_1$ , whereas the behavior at high doses is the same as that of  $m_1$ . The equilibrium value reached at high doses is significantly smaller; its simulated value is  $1.75 \times 10^{12} \text{ cm}^{-3}$ , nearly three orders of magnitude smaller than the maximum occurring at a dose of  $\sim 10^{16} \text{ cm}^{-3}$ . This behavior of a significant decline in the OSL intensity resembles that reported by Freytag,<sup>4</sup> Tesch,<sup>5</sup> and Böhm *et al.*<sup>6</sup>

#### IV. DISCUSSION

The obvious relation between  $m_1$  at the end of relaxation, at the end of stimulation, and the integral of the OSL has been explained above with relation to Fig. 2. The non-monotonic dose dependence of the integral OSL has been previously<sup>14</sup> associated with competition during either excitation or readout (or, perhaps, both). In the present simulation,  $m_1$  (Fig. 2) is decreasing with the dose and  $n_1$  is increasing with the dose, and therefore, obviously, competition during excitation is not the leading factor for the non-monotonic dependence. Competition during readout may have an important role; however, the apparent effect may be explained in a different way as follows. On p. 169 of Ref. 1, it is shown that for TL, the area under the glow peak depends on  $\min(n_0, m_0)$ , where  $n_0$  and  $m_0$  are, respectively, the occupancies of active traps and centers at the end of irradiation and prior to heating. The same considerations hold for  $n_1$  and  $m_1$  at the end of excitation in the present case of integral OSL. Considering Fig. 3, it is obvious that at relatively low

doses,  $n_1 < m_1$ , and therefore, the simulated OSL behaves like  $n_1$  (curve b), i.e., increasing with the dose. In fact, since OSL is given in the same units as the concentration, the two curves practically coincide at low doses. At high doses,  $n_1 > m_1$ , and therefore, the OSL (curve c) behaves like  $m_1$  (curve a), namely, decreases with the dose, and at high enough doses, the two curves coincide. One might expect that the maximum will occur when  $n_1 = m_1 \approx 2 \times 10^{15}$ . In fact, the maximum signal occurs at a dose of  $\sim 10^{17}$ , whereas the maximum OSL takes place at  $\sim 1.6 \times 10^{17}$ . This slight discrepancy should be attributed to nontrivial dynamic effects that have to do with the variations which take place in  $n_2$  and  $m_2$  in the same dose range.

As for the results of Fig. 4, where the radiative recombination center  $m_1$  is initially nil, curve (a) for the concentration of these centers and (c) for the OSL are similar, peak-shaped functions, but not identical. The similarity between the curves points to an effect of competition during excitation. The slight shift of the OSL peak to higher doses than that of  $m_1$  can be explained, taking into consideration the  $n_1$  curve (b) which is an increasing function at the same dose range. Roughly speaking, the integrated OSL can be considered as the product of  $n_1$  and  $m_1$  and when a peak-shaped function is multiplied by an increasing function, the result is usually a peak-shaped function, the maximum of which occurring at higher values of the argument.

We would like to discuss now the nonzero plateau values of the OSL, which are not saturation values, observed at high doses both in some experimental results as mentioned above and in Figs. 2–4 as a result of the simulations. For illustration, let us start by considering the set of parameters yielding Figs. 2 and 3. Note that at high doses, the simulation yielded an equilibrium value of  $3.7 \times 10^{14}$  for  $m_1$ , from which the same value was found for the OSL, and  $1.303 \times 10^{16}$  for  $m_2$ . We will show now how these values are associated with the set of parameters chosen for the simulation. Note that initially, we have  $m_{10} = 9.4 \times 10^{15}$ . This necessarily means that there is another entity in the sample, an entirely disconnected trapping state that does not participate in the exchange of carriers during excitation or readout, but should be assumed to exist due to neutrality considerations and hold  $9.4 \times 10^{15}$  electrons. During a given excitation, the same number of electrons is accumulated in  $N_1$  and  $N_2$  as holes in  $M_1$  and  $M_2$ , and those accumulated in  $M_1$  and  $M_2$  are in addition to the initial  $m_{10}$  mentioned above; therefore if we consider points in time following excitation, we have

$$n_1 + n_2 + 9.4 \times 10^{15} = m_1 + m_2. \quad (14)$$

If we consider high enough dose such that both  $N_1$  and  $N_2$  are saturated, a situation that can take place only if  $N_1 + N_2$  is smaller than  $M_1 + M_2$ , then we can write for this range

$$N_1 + N_2 + 9.4 \times 10^{15} = m_1 + m_2. \quad (15)$$

The mentioned nonzero plateau results from a state of dynamic equilibrium in which the net change of both  $m_1$  and  $m_2$  is nil. In other words, the number of holes trapped per second in each center is equal to the number of holes recombining with electrons in the same center per second, i.e.,

$$A_{m_1} m_1 n_c = B_1 (M_1 - m_1) n_v, \quad (16)$$

$$A_{m_2} m_2 n_c = B_2 (M_2 - m_2) n_v. \quad (17)$$

Dividing the two equations by one another, one gets

$$\frac{A_{m_1} m_1}{A_{m_2} m_2} = \frac{B_1 (M_1 - m_1)}{B_2 (M_2 - m_2)}. \quad (18)$$

With the given set of parameters, Eqs. (15) and (18) are two equations in the two unknown parameters  $m_{1e}$  and  $m_{2e}$ , the equilibrium values of the centers concentration, which can be solved, say, by inserting  $m_{2e}$  from Eq. (15) into (18), thus yielding a quadratic equation in  $m_{1e}$ . Out of the two possible solutions, one is found to be negative, and therefore, non-physical. The positive equilibrium value is  $\sim 3.7 \times 10^{14} \text{ cm}^{-3}$ , which is exactly the plateau level seen on the right-hand side of curves (a) and (c) of Fig. 2. The equilibrium value of the competing center  $m_{2e}$  can immediately be found from that of  $m_{1e}$  using Eq. (15) and the value found is  $m_{2e} = 1.303 \times 10^{16} \text{ cm}^{-3}$ . It should be noted that this consideration applies to the equilibrium *during* excitation, and the relevant occupancies may be somewhat different at the end of relaxation. With the examples given here, however, it has been found that the additional contribution to the concentration of the traps and centers is minor, less than 1%, and therefore, the evaluated numbers are valid.

A similar calculation can be made for the situation in which the initial filling of the radiative center is zero, as shown in Fig. 4. Here, the left-hand side of Eq. (15) includes only  $N_1 + N_2$ , or  $4 \times 10^{15} \text{ cm}^{-3}$  with the given parameters. Solving the analog of Eq. (15) with this value along with Eq. (18) yields  $m_{1e} = 6.13 \times 10^{13} \text{ cm}^{-3}$ , which is the plateau level shown in curves (a) and (c) of Fig. 4. The resulting value for  $m_{2e}$  is  $3.94 \times 10^{15} \text{ cm}^{-3}$ . A similar calculation performed for the parameters yielding Fig. 5, namely, the same as in Fig. 3 but with  $M_2 = 2.4 \times 10^{18} \text{ cm}^{-3}$ , yielded  $m_{1e} = 1.75 \times 10^{12} \text{ cm}^{-3}$  which, indeed, is the value reached for high doses in

Fig. 5. This value is more than three orders of magnitude smaller than the maximum of the scale, and therefore looks like zero on the figure.

In conclusion, the present work has shown, using simulations as well as intuitive physical considerations, the main features seen in the dose dependence of integral OSL, namely, the occurrence of a peak-shaped curve followed by an equilibrium plateau at high doses, in the framework of a model with two trapping states and two kinds of recombination centers. The relation between the concentrations of the active center at different stages of the process and the OSL integral has been discussed. Also, the direct connection between the relevant parameters chosen for simulation and the high dose equilibrium value has been established.

<sup>1</sup>R. Chen and S. W. S. McKeever, *Theory of Thermoluminescence and Related Materials* (World Scientific, Singapore, 1997).

<sup>2</sup>J. L. Lawless, R. Chen, D. Lo, and V. Pagonis, *J. Phys.: Condens. Matter* **17**, 737 (2005).

<sup>3</sup>J. H. Schulman, H. W. Etzel, and J. G. Allard, *J. Appl. Phys.* **28**, 792 (1957).

<sup>4</sup>E. Freytag, *Health Phys.* **20**, 93 (1983).

<sup>5</sup>K. Tesch, *Radiat. Prot. Dosim.* **6**, 347 (1983).

<sup>6</sup>M. Böhm, E. Pitt, and A. Scharmann, *Radiat. Prot. Dosim.* **8**, 139 (1984).

<sup>7</sup>D. Zeneli, M. Tavlet, and F. Coninckx, *Radiat. Prot. Dosim.* **66**, 59 (1996).

<sup>8</sup>D. Bloom, D. E. Evans, S. A. Holmstrom, J. C. Polf, S. W. S. McKeever, and V. Whitley, *Radiat. Meas.* **37**, 141 (2003).

<sup>9</sup>E. G. Yukihara, V. H. Whitley, J. C. Polf, D. M. Klein, S. W. S. McKeever, A. E. Akselrod, and M. S. Akselrod, *Radiat. Meas.* **37**, 627 (2003).

<sup>10</sup>S. W. S. McKeever, M. S. Akselrod, L. E. Colyott, N. Agersap Larsen, J. C. Polf, and V. Whitley, *Radiat. Prot. Dosim.* **84**, 163 (1999).

<sup>11</sup>E. G. Yukihara, V. H. Whitley, S. W. S. McKeever, A. E. Akselrod, and M. S. Akselrod, *Radiat. Meas.* **38**, 317 (2004).

<sup>12</sup>E. G. Yukihara, R. Gaza, S. W. S. McKeever, and C. G. Soares, *Radiat. Meas.* **38**, 59 (2004).

<sup>13</sup>V. Pagonis, R. Chen, and J. L. Lawless (unpublished).

<sup>14</sup>V. Pagonis, R. Chen, and J. L. Lawless, presented at the 11th International Conference on Luminescence and ESR Dating, Köln, Germany, July 2005, *Radiat. Meas.* (in press).

<sup>15</sup>R. Chen and P. L. Leung, *J. Appl. Phys.* **89**, 259 (2001).

<sup>16</sup>M. Lax, *Phys. Rev.* **119**, 1502 (1960).